Anion–Cation Redox Competition and the Formation of New Compounds in Highly Covalent Systems

Jean Rouxel*

Abstract: The increase in energy of the sp anionic band on going from oxides to the less electronegative sulfides, selenides, or tellurides (with a similar trend in neighboring columns) facilitates anion–cation redox interactions involving the d levels of transition metal cations and the sp levels of anionic species. The interactions can induce phase transitions or gradual change within a given structural model. When a cation is reduced by electron transfer to its d levels from the sp band, holes appear at the top of the latter. Interesting soft chemistry can be carried out based on redox processes that neutralize the holes with electrons. This approach also allows particular structural types to be stabilized. Three structural domains can be recognized amongst the transition elements: 1) on the left-hand side of the periodic table layered structures are observed involving M^{4+} and $(chalcogen)^{2-}$ ions; 2) formation of sets of metal–metal bonds is then observed, the geometry of which depends on both the initial electron population and the electron transfer to the metal; 3) on the right-hand side the metals in their highest oxidation state are no longer active, and the holes at the top of the sp band are taken up by a catenation of the anions, which can lead to full polymerization of the anionic sublattice.

Keywords: chalcogenides · periodic trends · redox reactions · soft chemistry · transition metals

Introduction

Discussions of redox behavior in solid-state chemistry mostly refer to the oxidation states shown by the cations in a given structure. At best, the mutual stability of two cations is examined with respect to a possible electron exchange between them. The anion is considered to play a more passive role. In any case, a large fluctuation in charge at the anion is not expected even though the abrupt changes in charge distribution in a hard sphere model can be smoothed out through the mechanism of bond ionicity.

This way of thinking can be traced back to the significant developments in oxide and fluoride chemistry for which the hard sphere model remains for the most part valid. This model helps to simplify structural descriptions, and emphasizes the central role played by transition metal cations in determining magnetic properties and in the construction of the conduction band from their d orbitals. We have gradually become accustomed to describing structures in terms of coordination polyhedra built up around cations. In terms of electron energy, this corresponds to the anionic s and p levels forming a band whose upper edge is low-lying, and their interaction with the majority of the transition metal d levels is thus ruled out. Except for in the highest oxidation states, the d levels lie above the sp band and lead to very ionic states.

The top of the sp band in sulfur, selenium, and tellurium is higher in energy than that in oxygen. The same is true for chlorine, bromine, and iodine compared to fluorine. Also, on going from left to right along a period of transition elements, the d levels are lowered. Therefore, with an appropriate metal/nonmetal combination, strong interactions can take place between sp band and d cation levels, leading to complex structures in which the the anionic entities may be significantly modified by electron transfer to the cationic species. One of the best known examples of this d cation/sp anion redox competition is the transition from dichalcogenides with layered structures on the left-hand side of the periodic table to pyrites and marcasites on the right.

Let us start with layered dichalcogenides. Their structure results from a stacking of slabs (Fig. 1), which are built up from edge-sharing octahedra (TiS_2 type) or trigonal prisms (NbS_2–MoS_2 type). The d orbital levels, which are split in the classical patterns 3–2 and 1–2–2 (from low to high energy), respectively, are located between a valence band, essentially built up from s and p anionic levels and the corresponding cationic levels that have been pushed up in energy (Fig. 2). The degree to which these d levels are filled governs the properties of the solids. With

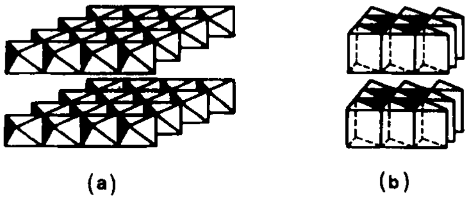

Fig. 1. The structure of layered chalcogenides: the stacked slabs are built up from a) octahedra sharing edges (TiS_2 type) or b) trigonal prisms (NbS_2 type).

---

[*] Jean Rouxel
Institut des Matériaux de Nantes, UMR CNRS No. 110
Université de Nantes
2, rue de la Houssinière, 44072 NANTES Cedex 03 (France)
Fax: Int. code + (40) 37-3995

0947-6539/96/0209-1053 $ 15.00+.25/0

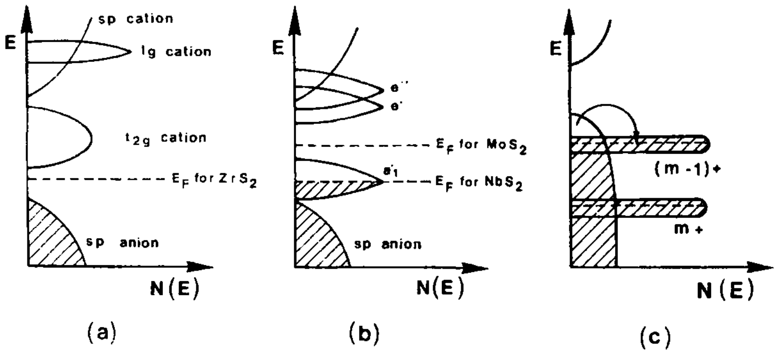

Fig. 2. Band-structure models for layered dichalcogenides: a) ZrS_2, TiS_2, b) NbS_2, MoS_2, and c) the drop in d-level energy on moving to the right-hand side of the periodic table, leading to a lowering of the oxidation state of the cation through an sp-to-d electron transfer.

empty d levels ZrS_2 (d^0) is a semiconductor. NbS_2 (d^1) shows a half-filled a'_1 band and metallic properties. With the same symmetry MoS_2 (d^2) has a filled a'_1 band and shows semiconducting behavior. On moving further to the right in the periodic table, the pyrite and marcasite structures appear. This is a direct consequence of the lowering of d levels along a period. At a critical point in the period the d levels will begin to overlap energetically with the valence band, and if they are initially empty, they will be filled at the expense of the valence band and holes will appear at the top of the latter. The holes may remain localized on specific anions, as we shall see below, but generally the anions condense in pairs to form $(S_2)^{2-}$, giving rise to pyrites or marcasite structure types. In chemical terms the cation has been reduced and the anion oxidized. We have moved, for example, from layered TiS_2 which is $Ti^{4+}\,2S^{2-}$ to FeS_2 with Fe^{2+} and $(S_2)^{2-}$ ions. This well-known transition was described as far back as 1968 by F. Jellinek.[1] We now know that it is in fact the most visible aspect of a much broader phenomenon concerned with variations in layered and pyrite structures, including metal clustering on the left-hand side of the periodic table and anion polymerization on the right. Significant changes in physical properties can be discussed in terms of the d–sp competition. The holes present at the top of a valence band also allow some interesting soft chemistry to be carried out, based on redox processes. Finally, new compounds can be stabilized by neutralizing holes with electrons to prevent the layer-to-pyrite transition from taking place. These points will be successively examined in this contribution. Previously published results will be reexamined,[2] and special attention will be paid to the soft chemistry that can be done with sp holes and to the stabilization of new structural types.

Discussion

1. Structural and electronic consequences of the d–sp redox competition on low-dimensional binary chalcogenides: Let us return to Figure 2. Chemistry allows us to play with the position of the top of the sp band as well as with the position of the d levels and the degree of filling of the sp band. The first of these adjustments involves comparing sulfides, selenides, and tellurides of a given cation. The three titanium dichalcogenides, for example, have the same CdI_2-type structure. With Ti^{4+} this would lead to an empty t_{2g} band and semiconducting properties. TiS_2 is indeed known to be a semiconductor, but $TiSe_2$ is a semimetal, as is evidenced by the substantial pressure dependence of its Hall coefficient,[3] and $TiTe_2$ is a metal. The large decrease in electronegativity of the anion along this series results in a significant rise in the top of the sp band.[4] The d levels are at first well removed from the sp band, and then just skimming above it or already inside the band. In the last case ($TiTe_2$), it was estimated from Mulliken overlap population calculations that 0.38 electrons are transferred from tellurium to titanium. This transfer has important structural consequences. Because the top of the sp band, which has some antibonding character, is being depopulated, the Te–Te distances are shortened. Te–Te contacts of 3.77 Å are observed, which are shorter than the sum of the van der Waals radii of 4.0 Å. Conversely, the existence of short anion–anion contacts in a given structure may be indicative of an electron transfer to d cationic levels, which may often explain unexpected physical properties such as electron conductivity or the magnitude of the magnetic moments.

Niobium triselenide is probably the best example in this context. The structure[5–6] is built up from individual $NbSe_3$ chains that run parallel to the *b* axis of a monoclinic unit cell. Each chain consists of stacked $[NbSe_6]$ irregular trigonal prisms, each containing an Se–Se bond in its base. Adjacent chains are displaced by *b*/2 (Fig. 3, top). As in most transition metal trichalcogenides one would expect the $M^{4+}X^{2-}(X_2)^{2-}$ charge distribution with M^{4+} cations surrounded by X^{2-} and $(X–X)^{2-}$ anions. This is indeed the situation in NbS_3,[7] which contains only one type of chain with Nb^{4+} cations, S^{2-} anions, and true $(S_2)^{2-}$ pairs ($d_{\text{S-S}} = 2.05$ Å). The d^1 electron configuration is responsible for Nb–Nb interactions along the chain. In the case of

Editorial Board Member:[*] *Jean Rouxel was born in Malestroit (France), studied chemistry in Rennes and obtained his Ph. D (Thèse d'Etat) under the guidance of P. Hagenmuller at the University of Bordeaux in 1961. He moved to Nantes in 1963 to found the laboratory of Solid State Chemistry and became Professor at the Institut Universitaire de France in 1991. Jean Rouxel has been president of the committee for Solid State Chemistry and Metallurgy and President of the Department of Chemistry at CNRS. He has received several awards and is a member of the French Academy of Sciences and of various foreign Academies (American Academy of Arts and Sciences, Indian National Academy, Academia Europaea). His major areas of scientific interest are 1) the synthesis of new phases, especially low-dimensional solids and phases formed by "chimie douce" processes, 2) understanding the chemical bond, through the observation of fluctuations in bonding (charge density waves) in inorganic chains and through the study of anions–cation redox competition, and 3) the description of the reactivity of solids in terms of their band structures and basic concepts. He has published over 270 papers and 7 patents. He has been editor/author of two books on the crystal chemistry of one-dimensional compounds and soft chemistry.*

---

[*] Members of the Editorial Board will be introduced to the readers with their first manuscript.

0947-6539/96/0209-1054 $ 15.00+.25/0

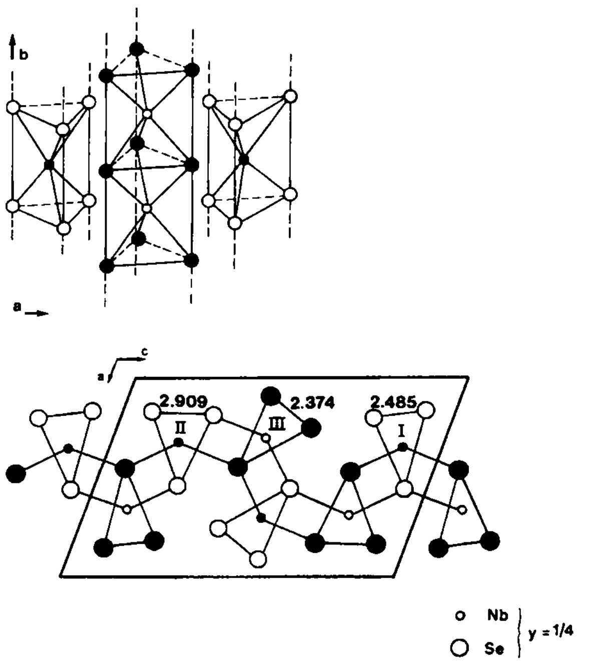

Fig. 3. Structure of niobium triselenide: top: adjacent [$NbSe_3$] chains are displaced by $b/2$; bottom: the three types of $NbSe_3$ chains.

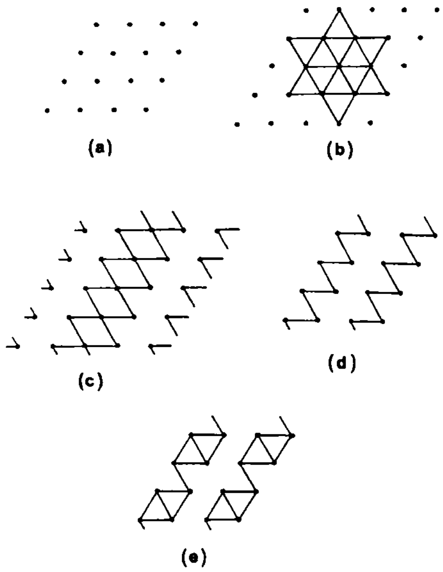

Fig. 4. Cluster formation in the slabs of 2D chalcogenides: a) undistorted hexagonal lattice typical for d^0 systems, b) metal-atom clustering typical for d^1 systems, c) double zig-zag chains found for d^2 systems, d) pattern in VTe_2, and e) metal-metal bonds in ReS_2 (d^3).

$NbSe_3$, there are three types of chains with three different values of the Se-Se bond lengths in the pairs (2.37, 2.49, 2.91 Å, respectively; Fig. 3, bottom). The value 2.37 Å in chain III corresponds to a true $(Se_2)^{2-}$ ion. Niobium in this chain is in the + IV oxidation state (d^1); this leads to a half-filled d_{z^2} band along the chain. Chain II can be regarded as insulating. Chains I and III bear the two charge density waves observed in $NbSe_3$,[8] as shown by the associated structural distortions. The Se-Se distances in chains I and II are much longer; this implies a partial population of the antibonding states. Depending on its length, that is, on the population of its antibonding states, the chalcogen dimer can behave as an electron reservoir, which governs the electronic properties of the adjacent metallic chains. Indeed the structural distortion is directly related to the electron population of the conduction band. It is characterized by a $\boldsymbol{q}$ vector which is equal to twice the Fermi vector ($\boldsymbol{q} = 2\boldsymbol{k}_F$).

Of course, instead of adjusting the top of the sp block, we can also lower (or raise) the position of the d levels by substituting a given metallic element with one that is less (or more) electropositive. The d levels in $HfTe_2$ are higher in energy than those in $TiTe_2$, and there is no electron transfer from Te to Hf. The Te-Te separation in $HfTe_2$ is consistent with the sum of the van der Waals radii.[9-10] In contrast (see above), electrons are transferred from Te to Ti in $TiTe_2$. The trend of increasing d-level energies down a column of the periodic table accounts for the stabilization of layered structures for the bottom elements, while pyrites and marcasites already start appearing for the top elements: MnS_2 is a pyrite, but ReS_2 is a layered compound.

ReS_2 is in fact a particularly interesting layered dichalcogenide. At the center of the [SReS] sandwiches making up the slabs there is a set of metal-metal bonds (Fig. 4e).[11] This is a classical situation which characterizes dichalcogenides of metals with d^1, d^2, and d^3 configurations. The d electrons may be used in the formation of metal-metal bonds at lower temperatures.[12-17] However, here again, the situation may differ for the tellurides and sulfides of a given element. In VTe_2 (Fig. 4d), there is an electron transfer of 0.25 electrons from Te to V,[4] which leads to a d^{1+x} configuration in the metal. This results in a particular superlattice arrangement of V-V bonds that is different from the d^1 pattern (Fig. 4b) and resembles the d^2 situation (Fig. 4c). The electrons that originate from the top of the mostly anionic sp band and which possess π-antibonding character now take part in the formation of a net of metal-metal σ bonds. The geometry and number of these bonds depend on the occupation of the d orbitals and on whether the electrons originate from the metal or are transferred from anions. Additional studies are needed to correlate x in d^{1+x}, d^{2+x} or d^{3+x} to particular bonding patterns. Nevertheless, anions, or at least the less electronegative ones, play a role in the two-dimensional clustering of the metal atoms within the slabs.

2. Soft chemistry with sp holes: When holes created at the top of an sp band do not associate, that is, anion pairing does not occur, the control of their population can lead to a very rich soft chemistry based on redox processes. The chemistry of copper thiospinels is a classic in this respect. Let us first consider $CuCr_2S_4$.[18] Polarized neutron studies as well as investigations by XPS led to the formulation $Cu^+(Cr^{3+})_2(S^{2-})_3S^{\cdot -}$. Chromium is in the + III oxidation state, and there is one hole on the anions per formula unit. The hole is delocalized in the anionic sublattice and leads to p-type metallic conductivity. It is also responsible for the strong ferromagnetic coupling between Cr^{3+} ions. The hole can easily be "neutralized" by one electron introduced through a reductive electrochemical intercalation of an additional copper in the $CuCr_2S_4$ framework [Eq. (1)]. Starting from

$$Cu^+ + e^- + Cu^+(Cr^{3+})_2(S^{2-})_3S^{\cdot -} \longrightarrow (Cu^+)_2(Cr^{3+})_2(S^{2-})_4 \qquad (1)$$

a ferromagnetic metal, one obtains a paramagnetic semiconductor. There is no longer a hole at the top of the sp band. An analogous spinel structure with the electronic arrangement $Cu^+(Cr^{3+})_2(Se^{2-})_3Br^-$ is adopted in $CuCr_2Se_3Br$.[19] In this example no additional copper can be intercalated, although the same geometrical possibilities are offered by the framework. This confirms the central role played by the sp hole in this type of reaction.

The reverse reaction, that is, the removal of copper from $CuCr_2S_4$, has been attempted. One expects to get a layered CrS_2 with a $CdCl_2$ structure in conjunction with the $(ABC)_n$ type of stacking of the anions in the spinel structure. These attempts have been unsuccesful (SCrS sandwiches would lie parallel to the 111 plane of the spinel structure). Removing copper would oxidize chromium to Cr^{4+} ions or create an additional hole. Both situations are unstable. Cr^{4+} has never been observed in the presence of sulfur. Two holes at the top of the sp band of sulfur (one hole for two sulfide ions) are not stable either. The top of the sp band is high enough to destabilize Cr^{4+}, but not to stabilize a high concentration of holes. The latter point seems to be supported by the fact that it has been possible to obtain layered $CrSe_2$ by deintercalating $KCrSe_2$ [Eq. (2)],[20] which has

$$KCrSe_2 - K^+ - e^- \longrightarrow Cr^{3+}Se^{2-}Se^{\cdot -} \qquad (2)$$

an $\alpha NaFeO_2$ structure with K^+ ions between $CrSe_2$ layers of edge-sharing $[CrSe_6]$ octahedra. The structure of the product is most likely $Cr^{3+}Se^{2-}Se^{\cdot -}$ with one hole on the anionic sublattice and Cr^{3+} ions. The fact that this reaction, which also leads to one hole for two chalcogenide ions, is now observed has certainly got something to do with the better stabilization of holes at the top of the much higher selenide sp band. Deintercalation of copper from $CuCr_2S_4$ could also result in the two holes forming a pair according to Equation (3). An IrS_2 type of structure would result. This has not been observed.

$$CuCr_2S_4 \longrightarrow Cu^+ + e^- + (Cr^{3+})_2(S^{2-})_2(S_2)^{2-} \qquad (3)$$

While $CuCr_2S_4$ is best described as an anionic mixed-valence system, in $CuTi_2S_4$ mixed valency occurs in the metal cations. The titanium d levels are high enough to stabilize the + IV oxidation state of the metal. The electronic structure is $Cu^+Ti^{3+}Ti^{4+}(S^{2-})_4$. Removal of copper simply results in oxidation of Ti^{3+} to Ti^{4+} (which is perfectly stable in the presence of sulfur). So-called cubic TiS_2 is formed, which has the $CdCl_2$ type of structure.[21–22] The difference between the "chimie douce" (soft chemistry) of $CuTi_2S_4$ and $CuCr_2S_4$ is simply explained by the change in position of d levels with respect to the top of the sp band. The difference between the "chimie douce" of $NaCrSe_2$ and $CuCr_2S_4$ (or similarly $NaCrS_2$) is due to the increase in energy of the top of the sp band. In both $CuTi_2S_4$ and $KCrSe_2$ deintercalation is possible because a higher oxidation state can be reached on the metal (TiS_2 case) or because holes on the anions can be stabilized ($CrSe_2$ case).

Let us select a few other examples among the many that have recently been reported, before discussing a case in which both cations and anions are oxidized. Thallium–copper sulfides and selenides represent a very interesting series of phases,[23–24] which can be described in terms of various structures of interweaving $TlCu_2X_2$ slabs and more copper-rich slabs.[25] Semiconducting phases like $TlCu_3Se_2$, which is $Tl^+(Cu^+)_3(Se^{2-})_2$, allow a deintercalation of copper from copper-rich slabs through "chimie douce" processes.[26] This can be achieved by electrochemistry, but also very directly and simply by using an aqueous ammonia solution.[27] $TlCu_2Se_2$ is obtained, which can be formulated as $Tl^+(Cu^+)_2Se^{2-}Se^{\cdot -}$. Similarly, $TlCu_2S_2$ is obtained from $TlCu_3S_2$. In fact, "chimie douce" is the only way to synthesize the latter compound. The deintercalated phases are metallic.[27]

The alkali metal (Na to Cs) copper chalcogenides[28–29] certainly show a comparable variety. In the case of potassium and sulfur,[28] for example, one finds $K_2Cu_8S_6$, $K_3Cu_8S_6$, and $K_3Cu_9S_6$. The structures are based on layers or chains built up from $[CuS_4]$ tetrahedra. The alkali metal is located between these units. $K_2Cu_8S_6$ is an anionic mixed-valence compound, which can be written as $(K^+)_2(Cu^+)_8(S^{2-})_4(S^{\cdot -})_2$. With only one hole on the anionic sublattice, $K_3Cu_8S_6$, formulated as $(K^+)_3(Cu^+)_8(S^{2-})_5S^{\cdot -}$, is a two-dimensional metal showing instabilities possibly of the charge density wave type.[30–31]

TlV_5S_8 is a tunnel-type chalcogenide.[32] Removing thallium from the tunnels results in an oxidation of the anionic sublattice with the formation of anionic mixed-valence states [Eq. (4)].

$$Tl^+(V^{3+})_5(S^{2-})_8 \longrightarrow (V^{3+})_5(S^{2-})_7S^{\cdot -} + Tl^+ + e^- \qquad (4)$$

Li_2FeS_2 is a more complicated case. The deintercalation of lithium proceeds in two steps, namely, an oxidation of Fe^{2+} to Fe^{3+} followed by the formation of anionic pairs. $Fe^{3+}S^{2-}(S_2)^{2-}_{1/2}$ is formed, which may be related to the IrS_2 structure. However, the poor crystallinity of the samples did not allow a precise structure determination. The above structural information was obtained by Mössbauer studies as well as IR and Raman spectra.[33]

The latter example shows that in deintercalation reactions it is necessary to carefully check that the resulting compound really retains the framework of the starting material. When transition elements of the left-hand side of the periodic table are present they can generally adopt a higher oxidation state, and a direct continuity is observed from the precursor to the final product (compare cubic TiS_2 and $CuTi_2S_4$ spinel). On the right-hand side d levels are deep in the sp band. Anionic pairs can be generated which may modify the framework. When a cation is oxidized it may also prefer another type of site in a given framework.

Finally, it should be mentioned that an appropriate substitution in the cationic sublattice may allow sulfur p-band holes to be generated, which induce p-type conductivity. A good example of this is β-$BaCu_2S_2$.[34] It shows a two-dimensional structure with $[Cu_2S_2]^{2-}$ anionic slabs separated by Ba^{2+} layers ($ThCr_2Si_2$ type). The preparation of the substituted phase $K_xBa_{1-x}Cu_2S_2$[35] leads to p-type conductivity. The compensation of charge cannot be achieved through an oxidation of some of the Cu^+ ions to Cu^{2+}. It is therefore taken up by the anionic sublattice and can be expressed by the formulation $(K^+)_x(Ba^{2+})_{1-x}(Cu^+)_2(S^{2-})_{2-x}(S^{\cdot -})_x$. One hole is introduced at the top of the sp band for each potassium, which allows an interesting variation in the physical properties.

3. Association of holes—anionic polymerization: The $(X_2)^{2-}$ species which are present in the pyrite and marcasite structures represent the simplest case of anion association. Much more complex anion patterns can be formed, the most extreme form of which is a full polymerization of the anionic sublattice. Even in the pyrite-type chalcogenides the classical bond length for S–S (≈ 2.06 Å), Se–Se (≈ 2.35 Å), and Te–Te pairs (≈ 2.75 Å) can be modified as a function of the position of the cation along a row of the periodic table. The variation of S–S distances along a period for a sulfide pyrite phase has been discussed in terms of an interaction between cationic e_g levels (low-spin octahedral), which are now low enough in energy, and π^* anionic states.[36] There is a shortening of the S–S distances from FeS_2 to CuS_2 with a concomitant reduction of the cation oxidation state. CuS_2 is in fact $Cu^+(S_2)^-$. The effect is similar to that described in Section 1 for the layered phases. It is magnified in the case of tellurides. $MnTe_2$ is probably the only telluride that contains true $(Te–Te)^{2-}$ pairs.[37]

Ir_3Te_8 and $CrTe_3$ represent an intermediate situation between compounds containing isolated $(Te_2)^{2-}$ pairs and those with a polymerized anionic sublattice. Ir_3Te_8 has a pyrite structure[38] with a random distribution of Ir^{3+} on the cation sites. Te_2 pairs do exist with a Te–Te distance of 2.833 Å, a bit longer than the value of 2.79 Å observed in $MnTe_2$. However, an analysis of all the distances shows that there are some distances between Te_2 pairs of 3.56 Å, much shorter than the nonbonding distance of 4.03 Å corresponding to the sum of van der Waals radii. Each tellurium of a pair is bonded to two others belonging to the same irridium coordination octahedron. This means that we are looking at some type of polymeric tellurium network, even though discrete Te–Te pairs (2.83 Å) can be identified. The balance of charges is not easy to express in such a compound. Clearly, the longer Te–Te distances, which result from complex equilibria between pairs, means that there is a higher formal charge on the pairs, necessary to compensate for nine cationic charges. Except for $MnTe_2$ (see above), where true $(Te_2)^{2-}$ pairs are separated by distances of the order of the sum of van der Waals radii, the transition metal ditellurides all show a range of Te–Te bond lengths.

$CrTe_3$ contains both $(Te_2)^{2-}$ and $(Te_3)^{2-}$ groups. The structural work by Klepp and Ipser[39] shows a layered structure with slabs built up from groups of four edge-linked $[CrTe_6]$ octahedra, which are connected via apical tellurium atoms. These building blocks are linked together through Te–Te bonds, giving rise to Te_2 and Te_3 entities. The very stable Cr^{3+} ions that are present impose a mean oxidation state of − I on the tellurium anions, and the charge balance can be viewed as $(Cr^{3+})_2(Te^{2-})(Te_2)^{2-}(Te_3)^{2-}$. Within the polyanions interatomic distances are 2.816 and 2.824 Å for $(Te_3)^{2-}$ and 2.817 Å for $(Te_2)^{2-}$. These are a bit longer than expected; this suggests higher charges on tellurium, assuming these groups are really isolated. In fact, within the sheets, Te–Te distances of 3.437 and 3.507 Å are observed, which indicate the presence of bonding. The distances of 3.85 Å between slabs are close enough to the sum of the van der Waals radii to exclude any bonding. $CrTe_3$ is a layered structure with in-plane anionic polymerization, although discrete Te_2 and Te_3 groups are clearly visible.

$IrTe_2$ does not have the pyrite structure as do some other ditellurides of the late transition elements. Until recently it was reported to have a CdI_2 structure.[40–41] Assuming the usual configuration, a Ir^{4+} oxidation state is implied, which is not acceptable. The same structural type has been reported for other ditellurides of the late transition elements.[41–43] But it is very unlikely that $CoTe_2$, for example, would adopt a CdI_2-like structure, since the corresponding sulfide is already a pyrite. As tellurium is less electronegative than sulfur, the top of its sp band is higher, and the d–sp redox competition is thus facilitated. We therefore expect $IrTe_2$ to have a pyrite structure. It appears that its structure was originally assigned only on the basis of similarities of powder diffraction patterns. The structure of $IrTe_2$ has since been redetermined[44] and is indeed of the CdI_2 type (*P*-3*m*1 space group). However, it was found that the tellurium atoms located at different elevations ($^1/_4$ and $^3/_4$) were bonded to each other (d_{Te-Te} = 3.497 and 3.558 Å), whereas nonbonding anions at the same level were found at 3.928 Å. Figure 5 compares $IrTe_2$ with $HfTe_2$, which represents an ideal CdI_2-type ditelluride. The extensive bonding between tellurium atoms within the slabs, and also between them, explains the rather short *c*/*a* ratio of 1.37 in the former, compared to the usual value of around 1.66 in a clasical CdI_2 structure. What we have here is an infinite polymerization of the anionic sublattice. These structures have been called polymeric CdI_2 structures. The short *c*/*a* ratio associated with the *P*-3*m*1 space group is indicative of this situation.

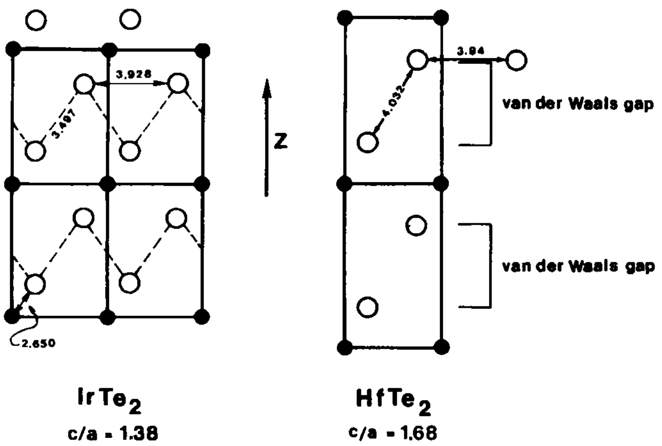

Fig. 5. Right: regular CdI_2 structure of $HfTe_2$. Left: polymerized CdI_2 structure of $IrTe_2$ with short Te–Te contacts between slabs leading to a reduced *c*/*a* ratio (1.38 instead of 1.68).

4. The role of electron transfer in structural stabilization—interweaving in highly covalent systems: Neutralizing holes at the top of an sp band by adding electrons from a donor will of course prevent the formation of anion pairs and stabilize a low-dimensional arrangement. Owing to the instability of Cr^{4+} in the presence of sulfur, layered CrS_2 cannot be synthesized, not even by deintercalation using low-temperature soft chemistry. However, $[CrS_2]$ slabs of the TiS_2 type exist in $NaCrS_2$ where they are separated by layers of Na^+ cations ($\alpha NaFeO_2$ structural type). $NaCrS_2$ can be regarded as an intercalation compound of sodium in an hypothetical layered CrS_2. It is indeed isostructural with $NaTiS_2$, which is a true intercalation compound of TiS_2. In the $[CrS_2]$ slabs of $NaCrS_2$, chromium is in the + III oxidation state, but the electrons transferred from sodium neutralize the holes that would otherwise exist. The final outcome is similar in $NaTiS_2$ and $NaCrS_2$. However, in forming $NaTiS_2$ electrons are added to Ti d levels of TiS_2, whereas, in the case of $NaCrS_2$, the Na electrons refill the top of the sp band in already reduced CrS_2 slabs. The same considerations apply to the stabilization of CrS_2 or VS_2 slabs by addition of phosphorus[45] or silicon.[46] In $P_{0.20}VS_2$ phosphorus occupies tetrahedral holes between VS_2 slabs.[45]

The Ge_xNbTe_2 phases[47] represent a case of particular importance. $NbTe_2$ does not exist with the layered trigonal prismatic structure of NbS_2, but addition of germanium stabilizes this structural arrangement, although with particular features regarding structure and chemical bonding (Ge was chosen first instead of Si or P, because Nb and Te atoms are larger than, for example, V and S atoms, but it appears that Si, at least, also gives good results). Ge is located in an unusual site at the center of rectangles separating Te_6 prisms that are not occupied by Nb atoms (Fig. 6). In addition some of the Nb atoms are linked together to form metal–metal pairs through a common rectangular face between adjacent trigonal prisms. Other Nb atoms remain isolated and form ribbons that demarcate the domains in which M–M bonds exist. The sequence according to which these regions alternate as a function of Ge concentration is responsible for the commensurate or incommensurate modulation of the structures. With general formulation $NbGe_{\frac{1+n}{3+2n}}Te_2$, all these phases have slabs that result from the association of three types of ribbons. Ribbons a and b contain both Ge atoms and M–M pairs with opposite orientations. Ribbon c contains isolated M atoms. Ge is in the + II oxidation

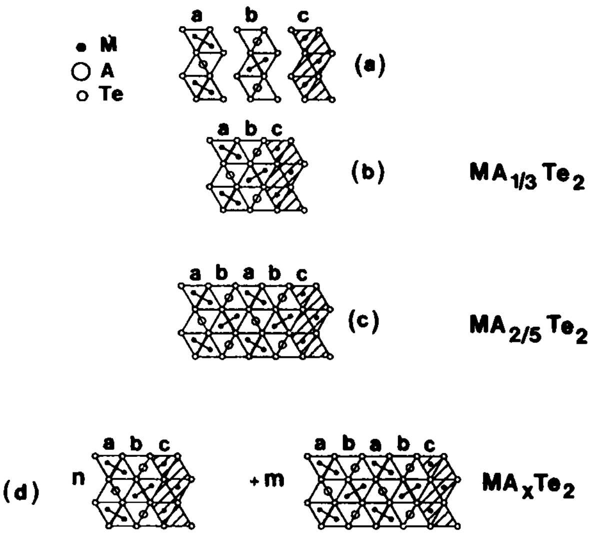

Fig. 6. a) The three ribbons (a, b, and c) used to construct an MA_xTe_2 slab (M = Nb, Ta; A = Si, Ge). Three examples of such constructions: b) $MA_{1/3}Te_2$, c) $MA_{2/5}Te_2$, and d) intermediate modulated compositions MA_xTe_2 ($^1/_3 < x < ^2/_5$).

state, as shown by an analysis of the density of states curves which reveals the presence of levels with Ge 4s character lying about 4 eV below the Fermi level, while the Ge 4p levels are well above E_f. Two electrons have been used to reduce Nb atoms. But niobium has also been reduced by electrons coming from the top of the tellurium sp band. Indeed the partial depopulation of these anionic states with antibonding character results in a $[Te_4]$ catenation. Two Te in one slab are associated with two in an adjacent one, through the van der Waals gap. Successive slabs are thus fixed relative to each other. In all compounds, the number of Ge atoms is equal to the number of Nb–Nb pairs. It could therefore be supposed that the two electrons donated by Ge are used by two Nb to form $(Nb^{3+})_2$ pairs. The other Nb atoms would be reduced through the transfer of electrons from the sp band. There is, however, no direct proof that such an hypothesis is correct. The interest in Ge_xNbTe_2 in the context of this contribution arises because both extra atoms (Ge, Si) act as donors and Te associations contribute to stabilize the structure.

The Ge_xNbTe_2 phases show a segregation of ribbons in a plane, that is, in a two-dimensional space. Misfit layered chalcogenides[48] represent a case of segregation of slabs in three-dimensional space. The presence of CrS_2 slabs in this series also relies on an electron transfer from a donor in adjacent slabs. With a general formulation $(MX)_{1+x}TX_2$ (M = Sn, Pb, Bi, Ln; X = S, Se; T = Ti, V, Nb, Ta, Cr), misfit layered chalcogenides present two-layer sublattices that alternate along a common axis (the *c* direction) (Fig. 7). The sublattice consists of octahedral (Ti, V, Cr) or trigonal prismatic (Nb, Ta) slabs similar to those of TiS_2 or NbS_2. The MX slab is a distorted 100 slice of the NaCl structure of the corresponding MX chalcogenides. The misfit is observed along one in-plane axis (*a* direction) and is directly reflected in the formulation $(MX)_{1+x}TX_2$ by the $1+x$ value, which is associated with the ratio of unit cells and ranges from 1.08 to 1.24. An important electron transfer takes place when MX is LnS. The electronic structure of this slab is $Ln^{3+}e^-S^{2-}$, like in rare earth monochalcogenides themselves. The electron is transferred to a CrS_2 slab, which is stabilized in the same way as described above in case of Si_xCrS_2 or $NaCrS_2$.

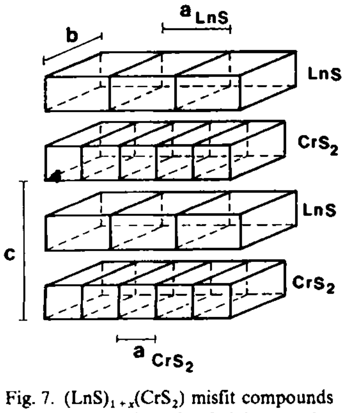

Fig. 7. $(LnS)_{1+x}(CrS_2)$ misfit compounds show an alternation of LnS slabs (pseudo-NaCl) and CrS_2 ones (TiS_2 type). Incommensurability occurs along *a*.

Conclusion

The very active role played by the anions in mostly covalent structures leads simultaneously to a great variety and a great complexity of effects. In the case of chalcogenides, which form the basis of our studies, one can envision three domains in the periodic table. On the left-hand side of a period of transition elements, simple layered structures are found with M^{n+} cations and X^{2-} anions. Further along, the destabilization of high oxidation states leads, at least for the elements in the second and third rows, such as Nb, Ta, Mo, W, or Re, to metal clustering within the layers. The geometry of such associations depends on the initial electron population on the metal and on the extra electrons transferred from the anions. Towards the right-hand side of the transition periods the d levels do not participate in anion-to-cation electron transfer processes. The anion simply absorbs the depopulation of the sp band through catenation. This catenation can range from simple $(X_2)^{2-}$ pairs in pyrites and marcasites to more complex groups that can eventually extend throughout the entire crystal (polymerized CdI_2 or pyrite structures).

With the depletion of antibonding levels, through electron transfer to the lower-lying cationic d levels, the anion–anion distance changes substantially. If the anion–anion distance is plotted versus the net charge per anion, a quasi-linear relationship is observed. For instance, if one considers $ZrTe_2$, with well-defined Te^{2-} ions, $MnTe_2$ with well-defined $(Te_2)^{2-}$ ions, and $IrTe_2$ with the Te_2^{3-} charge balance (i.e., $Te^{-1.5}$), the corresponding linear variation is shown in Figure 8. Many other examples that we have studied can be considered, with sulfides, selenides, and tellurides. It is not clear why such a linear relation exists.

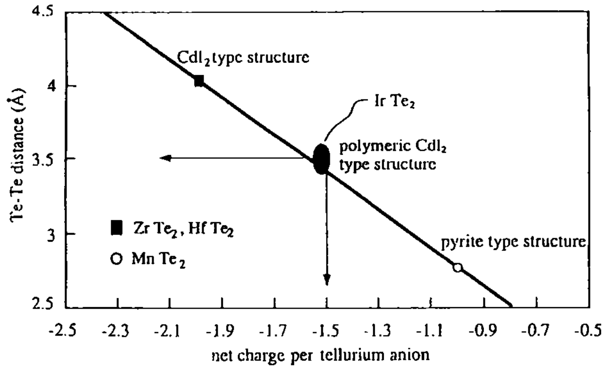

Fig. 8. Plot of formal oxidation state per tellurium atom versus Te–Te distances for a "regular" CdI_2 structure with isolated Te^{2-} ions ($ZrTe_2$, $HfTe_2$), a polymerized CdI_2 structure of $IrTe_2$ ($Te^{-1.5}$), and a true pyrite structure with $(Te_2)^{2-}$ pairs ($MnTe_2$).

A nice extension of the work described here would be to study the effect of pressure, which might lead to changes in the anion–anion distances. Other important questions that should be resolved are: "why can holes be found isolated at the top of a given band?" and "when do these holes associate to form an anionic catenation?". The problem is exactly analogous to that encountered for electrons located on cations.

The wealth of soft chemistry implied by the occurrence of those holes opens many new and promising prospects. There is a whole chapter on the chemistry of antibonds that remains to be written.

Received: March 15, 1996 [C 320]

---

[1] F. Jellinek, in *Inorganic Sulfur Chemistry* (Ed.: G. Nickless), Elsevier, Amsterdam, **1968**.

[2] a) S. Jobic, R. Brec, J. Rouxel, *J. Solid State Chem.* **1992**, *96*, 169. b) J. Rouxel, *Comments Inorg. Chem.* **1993**, *14 no. 4*, 207

[3] R. H. Friend, D. Jérome, W. Y. Liang, J. C. Mikkelsen, A. D. Yoffee, *J. Phys. C: Solid State Phys.* **1977**, *10*, L 705.

[4] E. Canadell, S. Jobic, R. Brec, J. Rouxel, M.-H. Whangbo, *J. Solid State Chem.* **1992**, *99*, 189.

[5] A. Meerschaut, J. Rouxel, *J. Less Common Met.* **1975**, *39*, 197.

[6] J. L. Hodeau, M. Marezio, C. Roucau, R. Ayroles, A. Meerschaut, J. Rouxel, P. Monceau, *J. Phys. C: Solid State Phys.* **1978**, *11*, 4117.

[7] J. Rijnsdorp, F. Jellinek, *J. Solid State Chem.* **1978**, *25*, 325.

[8] J. Chaussy, P. Haen, J. L. Lasjaunias, P. Monceau, G. Waysand, A. Waintal, A. Meerschaut, P. Molinié, J. Rouxel, *Solid State Commun.* **1976**, *29*, 759.

[9] F. Hulliger, in *Structural Chemistry of Layer Type Phases* (Ed.: F. Levy), D. Reidel **1976**, p. 222.

[10] G. Lucovsky, R. M. White, J. A. Benda, J. F. Revelli, *Phys. Rev. B* **1973**, *7*, 3859.

[11] J. C. Wilderwanck, F. Jellinek, *J. Less Common Met.* **1971**, *24*, 73.

[12] J. A. Wilson, F. J. DiSalvo, S. Mahajan, *Adv. Phys.* **1975**, *24*, 111.

[13] R. Brouwer, F. Jellinek, *Physica* **1980** *B99*, 51.

[14] E. Canadell, M.-H. Whangbo, *Inorg. Chem.* **1990**, *29*, 1398

[15] B. E. Brown, *Acta Crystallogr.* **1966**, *20*, 268.

[16] N. W. Alcock, H. Kjekshus, *Acta Chem. Scand.* **1965**, *19*, 79.

[17] K. D. Bronsema, G. W. Bus, G. A. Wiegers, *J. Solid State Chem.*, **1986**, *53*, 415.

[18] R. Schöllhorn, *Angew. Chem. Int. Ed. Engl.* **1988**, *27*, 1392.

[19] A. Payer, M. Schmalz, W. Paulus, R. Schlögl, R. Schöllhorn, *J. Solid State Chem.* **1992**, *98*, 71.

[20] C. F. Van Bruggen, R. J. Haange, G. A. Wiegers, D. K. G. de Boer, *Physica* **1980**, *99B*, 166

[21] R. Schöllhorn, A. Payer, *Angew. Chem. Int. Ed. Engl.* **1985**, *24*, 67.

[22] D. Murphy, S. Sinha, *Solid State Ionics* **1986**, *20*, 81.

[23] R. Berger, *Chem. Scripta* **1988**, *28*.

[24] R. Berger, L. Eriksson, A. Meerschaut, *J. Solid State Chem.* **1990**, *87*, 283; *ibid.* **1991**, *90*, 61.

[25] R. Berger, R. V. Bucur, *Mater. Res. Bull.* **1992**, *27*, 439.

[26] R. Berger, *J. Less Common Met.* **1989**, *147*, 141.

[27] R. Berger, C. F. Van Bruggen, *J. Less Common Met.* **1984**, *99*, 113.

[28] W. Rudorff, H. G. Schwarz, M. Walter, *Z. Anorg. Allg. Chemie* **1952**, *269*, 141.

[29] H. Schils, W. Bronger, *Z. Anorg. Allg. Chemie* **1979**, *456*, 187.

[30] L. W. ter Haar, F. J. DiSalvo, H. E. Bair, R. M. Fleming, J. V. Waszczak, *Phys. Rev. B* **1987**, *35–4*, 1932.

[31] R. M. Fleming, L. W. ter Haar, F. J. DiSalvo, *Phys. Rev. B* **1987**, *35–10*, 5388.

[32] W. Schramm, R. Schöllhorn, H. Eckert, W. Müller-Warmuth, *Mater. Res. Bull.* **1983**, *18*, 1283.

[33] L. Blandeau, G. Ouvrard, Y. Calage, R. Brec, J. Rouxel, *J. Phys. C* **1987**, *20*, 4271.

[34] J. E. Iglesias, K. E. Pachali, H. Steinfink, *Mater. Res. Bull.* **1972**, *7*, 1247.

[35] X. Zhang, T. Hogan, C. R. Kannewurf, M. G. Kanatzidis, *J. Alloys Compd.* **1996**, in press.

[36] J. C. W. Folmer, F. Jellinek, J. H. M. Calis, *J. Solid State Chem.* **1988**, *72*, 137.

[37] S. Jobic, R. Brec, J. Rouxel, *J. Alloys Compd.* **1992**, *178*, 233

[38] A. Kjekshus, T. Rakke, F. A. Andresen, *Acta Chem. Scand.* **1979**, *A33*, 719.

[39] K. O. Klepp, H. Ipser, *Angew Chem. Int. Ed. Engl.* **1982**, *21*, 911.

[40] E. F. Hocking, J. G. White, *J. Phys. Chem.* **1960**, *64*, 1042.

[41] R. M. A. Lieth, in *Crystallography and Crystal Chemistry of Materials with Layered Structures* (Ed.: F. Levy), **1977**, Vol. 1, D. Reidel.

[42] R. W. G. Wyckoff, *Crystal Structures* **1965**, Wiley N. Y.

[43] F. Hulliger, in *Structural Chem. of Layer Type Phases* (Ed.: F. Levy), **1976**, Vol. 5.

[44] S. Jobic, P. Deniard, R. Brec, J. Rouxel, A. Jouanneaux, A. Fitch, *Z. Anorg. Allg. Chemie* **1991**, *199*, 598.

[45] G. Ouvrard, R. Brec, J. Rouxel, *Ann. Chim. (Paris)* **1982**, *7*, 53.

[46] R. Brec, G. Ouvrard, S. Jobic, unpublished results.

[47] a) L. Monconduit, M. Evain, F. Boucher, R Brec, J. Rouxel, *Z. Anorg. Allg. Chem.* **1992**, *616*, 177. b) J. Li, E. Badding, F. J. DiSalvo, *J. Alloys Compd.* **1992**, *184*, 257. c) A. Van der Lee, M. Evain, L. Monconduit, R. Brec, V. Petricek, *Inorg. Chem.* **1994**, *33*, 3032. d) J. Rouxel, M. Evain, *Eur. J. Solid State Inorg. Chem.* **1994**, *31*, 683.

[48] For a general description see: a) J. Rouxel, A. Meerschaut, G. Wiegers, *J. Alloys Compd.* **1995**, *229*, 144–157. b) G. Wiegers, A. Meerschaut, in *Incommensurate Sandwiched Layered Compounds* **1992** (Ed.: A. Meerschaut), Trans. Tech. Publications, 104–172.